The EMBO Journal Vol.17 No.6 pp.1598–1605, 1998

Assembly mechanism of the oligomeric streptolysin O pore: the early membrane lesion is lined by a free edge of the lipid membrane and is extended gradually during oligomerization

Michael Palmer[1], Robin Harris[2], Claudia Freytag[3], Michael Kehoe[3], Jørgen Tranum-Jensen[4] and Sucharit Bhakdi

Institute of Medical Microbiology, University of Mainz, Augustusplatz, D-55101 Mainz, [2]Institute of Zoology, University of Mainz, Müller-Weg, Mainz and [3]Institute of Medical Microbiology, University of Magdeburg, Magdeburg, Germany, [3]Department of Microbiology, The Medical School, University of Newcastle upon Tyne, Newcastle upon Tyne NE2 4HH, UK and [4]Department of Anatomy, Panum Institute, University of Copenhagen, Blegdamsvej 3, DK 2200 Copenhagen, Denmark

[1]Corresponding author

Streptolysin O (SLO) is a bacterial exotoxin that binds to cell membranes containing cholesterol and then oligomerizes to form large pores. Along with rings, arc-shaped oligomers form on membranes. It has been suggested that each arc represents an incompletely assembled oligomer and constitutes a functional pore, faced on the opposite side by a free edge of the lipid membrane. We sought functional evidence in support of this idea by using an oligomerization-deficient, non-lytic mutant of SLO. This protein, which was created by chemical modification of a single mutant cysteine (T250C) with *N*-(iodoacetaminoethyl)-1-naphthylamine-5-sulfonic acid, formed hybrid oligomers with active SLO on membranes. However, incorporation of the modified T250C mutant inhibited subsequent oligomerization, so that the hybrid oligomers were reduced in size. These appeared as typical arc lesions in the electron microscope. They formed pores that permitted passage of NaCl and calcein but restricted permeation of large dextran molecules. The data indicate that the SLO pore is formed gradually during oligomerization, implying that pores lined by protein on one side and an edge of free lipid on the other may be created in the plasma membrane. Intentional manipulation of the pore size may extend the utility of SLO as a tool in cell biological experiments.

Keywords: pore-forming toxins/protein oligomerization/streptolysin O/thiol-activated toxins

Introduction

Streptolysin O (SLO) belongs to the homologous group of thiol-activated toxins (Alouf and Geoffroy, 1991) that are elaborated by various Gram-positive bacteria. These toxins bind as monomers to cholesterol in the cytoplasmic membranes of animal cells (Ohno Iwashita *et al.*, 1991). They then oligomerize into ring-shaped structures, estimated to contain 50–80 subunits (Bhakdi *et al.*, 1985; Sekiya *et al.*, 1993), which surround pores of ~30 nm diameter. This size by far exceeds that of most other proteinaceous pores, e.g. staphylococcal α-toxin (Fuessle *et al.*, 1981) or the complement membrane attack complex (Bhakdi and Tranum Jensen, 1984). SLO pores permit flux of both ions and macromolecules (Bhakdi *et al.*, 1985; Hugo *et al.*, 1986), and the toxin has thus become a popular tool for the controlled permeabilization of cell membranes (Bhakdi *et al.*, 1993).

Besides rings of varying diameter, incomplete arc-shaped forms are commonly seen on electron micrographs of SLO-treated erythrocyte membranes. Such arcs previously were observed to be accompanied by membrane defects that appeared to be lined by a free edge of the cell membrane (Bhakdi *et al.*, 1985). These observations have recently been accommodated into a working model of SLO pore assembly. In this model, SLO initially forms small arcs comprising very few subunits that insert into the membrane. The membrane lipids facing the concave side of the arc will retract to form a crescent-shaped membrane defect. The latter subsequently is extended by successive addition of further SLO monomers to the free ends of the arc, which will eventually give rise to the complete ring-shaped transmembrane pore. While this model accounts for both the electron microscopic data and the kinetics of SLO oligomerization (Palmer *et al.*, 1995), it has not yet been substantiated in functional terms. The proposed mechanism of pore formation is profoundly different from that of staphylococcal α-toxin, the hitherto best-studied bacterial pore-forming toxin. With the latter, oligomerization has been shown to precede membrane insertion and permeabilization (Walker *et al.*, 1992), which occurs as a cooperative event within the completely assembled pre-pore (Valeva *et al.*, 1997). A similar mechanism has been considered for the thiol-activated toxins (Rossjohn *et al.*, 1997). If, in contrast, SLO could be shown to follow the model of simultaneous oligomer and pore assembly outlined above, this would introduce a second mechanistic paradigm to the field of bacterial pore-forming toxins. The key to the resolution of these uncertainties lies in the experimental verification or negation of the contention that SLO pore formation commences at an early stage of oligomerization, and that the pore concomitantly grows in mass and functional size.

Here, we report on an oligomerization-deficient mutant protein that, through co-application with native SLO, allows the size of oligomers to be manipulated. Oligomers of reduced size can be generated that resemble the arc-shaped structures also observed with wild-type SLO. They permeabilize the target membrane, whereby a correlation of oligomer and pore size can be demonstrated. The results are clearly in favor of the novel mechanism of concomitant oligomer and pore formation. Equally significantly, they provide evidence that stable pores, which are lined by protein on one side and an edge of free lipid on the other, may be created in the plasma membrane.

Results

Specific hemolytic activity of mutant T250C

Residue T250 in the cysteine-less active SLO mutant C530A (Pinkney *et al.*, 1989) was replaced by cysteine to yield the (double) mutant T250C. The specific hemolytic activity of T250C was identical to that of the parent mutant C530A (hemolytic titer with a 1 mg/ml solution and 2.5% rabbit erythrocytes, 1:40 000). The mutant protein could be derivatized with the sulfhydryl-modifying reagent *N*-(iodoacetaminoethyl)-1-naphthylamine-5-sulfonic acid (IAEDANS) under native conditions with a yield of >90%. The hemolytic activity of the modified protein (T250C-AEDANS) was reduced to <0.1% of that before modification as judged by hemolytic titration. Apart from T250C and C530A, further mutants used in this work have been described previously (Palmer *et al.*, 1996). The single cysteines of these mutants (S101C and N218C, respectively) were used here solely as carriers of fluorescent or radioactive labels. These proteins fully retained their hemolytic capability after labeling (data not shown).

Modification of residue 250 by IAEDANS interferes with oligomerization

Pore formation by SLO occurs in two distinct steps: first, binding of the toxin monomer to membranes, and second, oligomerization of membrane-associated monomers. Accordingly, the abolition of hemolytic activity with T250C-AEDANS might be related to either step. When T250C-AEDANS was incubated with rabbit erythrocytes, the mutant toxin became largely depleted from the supernatant, which showed that its capacity to bind to cells essentially is preserved (Figure 1). The ability of T250C-AEDANS to form oligomers on membranes was characterized by the experiment shown in Figure 2. The protein was applied to liposomes containing cholesterol and incubated at 37°C to allow for oligomerization. The liposomes were solubilized with detergent and the sample analyzed by gel permeation chromatography on Sephacryl S300. While the lytic labeled mutant S101C (Palmer *et al.*, 1996), after incubation with liposomes, was recovered in oligomeric form in the exclusion volume, the T250C-AEDANS protein was eluted in the same fractions as the monomer control. The non-lytic phenotype of T250C-AEDANS, therefore, is related to oligomerization but not to membrane binding. However, when admixed with an equal amount of the active protein C530A, T250C-AEDANS protein became incorporated to a large extent into oligomers that must be hybrids of the two proteins (Figure 2). This finding indicates that kinetically distinct stages exist in the oligomerization process which must be differentially susceptible toward inhibition by the structural change in the T250C-AEDANS molecule.

Hybrid oligomers of T250C-AEDANS and active SLO are reduced in size

We next asked whether or not the above hybrid oligomers would grow to full size. The active SLO mutant C530A was mixed with varying amounts of T250C-AEDANS and incubated with rabbit erythrocytes. A small amount of the functionally active N218C SLO mutant, labeled with ^{125}I, was also included in the toxin mixture to facilitate quantitation of oligomers. The samples were

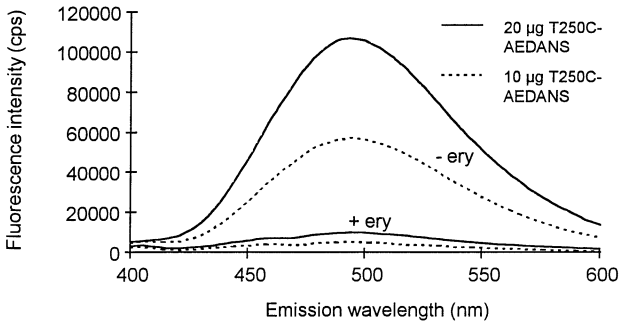

Fig. 1. The non-lytic IAEDANS derivative of the streptolysin O mutant T250C binds to cell membranes. The IAEDANS-derivatized mutant T250C (SLO T250C-AEDANS; final concentration 20 or 10 µg/ml) was incubated for 5 min on ice with 5% rabbit erythrocytes. The cells were pelleted by centrifugation, and the supernatant was assayed for AEDANS fluorescence. Comparison of the supernatants (+ery) with control samples without erythrocytes (–ery) shows that ~90% of the protein has been bound to the cells.

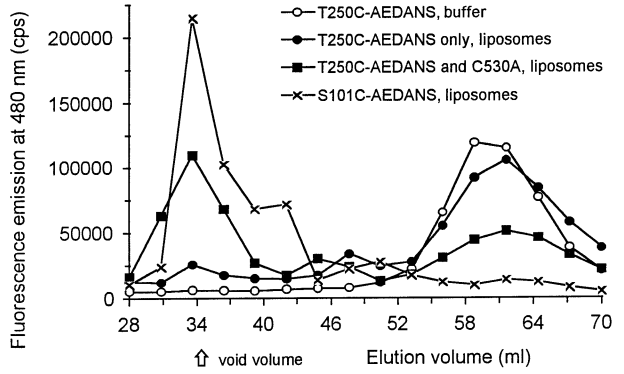

Fig. 2. T250C-AEDANS is incapable of initiating oligomerization but forms hybrid oligomers with native SLO. T250C-AEDANS (100 µg total) was incubated at 37°C with liposomes containing cholesterol. The sample was solubilized with Triton X-100 and chromatographed on Sephacryl S300; the column fractions were analyzed for AEDANS fluorescence. The mutant protein was eluted in the same fractions as the monomer control sample without liposomes, showing that no oligomerization of T250C-AEDANS had occurred. In contrast, a sample of the active mutant S101C-AEDANS, upon incubation with liposomes, yielded oligomers that were eluted in the void volume. If T250C-AEDANS was mixed with the active, unlabeled mutant C530A and incubated with liposomes, a major part of the label fluorescence was again recovered in the void volume, showing formation of hybrid oligomers from the two proteins.

then solubilized with detergent and subjected to density gradient centrifugation. Figure 3 shows the distribution of the ^{125}I-labeled protein in the gradients. The oligomers generated from C530A (and [^{125}I]N218C) toxin only were recovered as a narrow peak from the bottom fractions. In the presence of T250C-AEDANS, the oligomer peak moved towards the top of the gradient. This indicated that T250C-AEDANS had effected a reduction in size of the oligomers; their average size was inversely related to the amount of T250C-AEDANS employed. However, even when T250C-AEDANS was employed in a 4-fold excess over C530A, the remaining oligomer peak was clearly separated from that of monomeric SLO, indicating that oligomerization had not been completely abrogated.

Mechanism of oligomerization interference by T250C-AEDANS

It must be assumed that each subunit of the SLO oligomer is connected laterally to its neighbors through two different

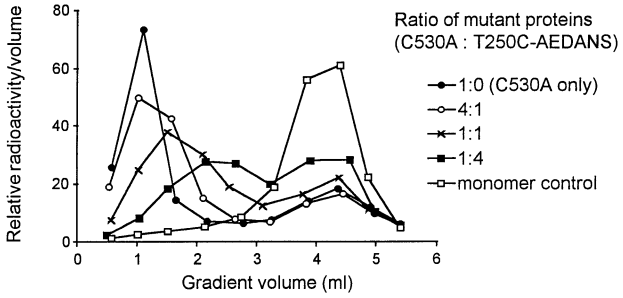

Fig. 3. Hybrid oligomers containing T250C-AEDANS are reduced in size. SLO T250C-AEDANS was admixed in various ratios to the lytically active mutant C530A, and the samples were supplemented with a small amount of another active mutant (S218C) labeled with ^{125}I. The protein mixtures were incubated with rabbit erythrocytes at 37°C to permit oligomerization. The cells were pelleted by centrifugation, solubilized with deoxycholate and centrifuged through deoxycholate/sucrose gradients. From each sample, 10 fractions were harvested and the radioactivity per volume was determined. The sample containing active SLO yielded only large oligomers that peaked in the bottom of the gradient. With increasing amounts of added T250C-AEDANS, the oligomer peak moved upward, reflecting reduction in oligomer average size. Even with the highest (4-fold) excess of T250C-AEDANS employed, the oligomer peak remained distinctly below the monomer peak, indicating that oligomerization had not been completely abrogated.

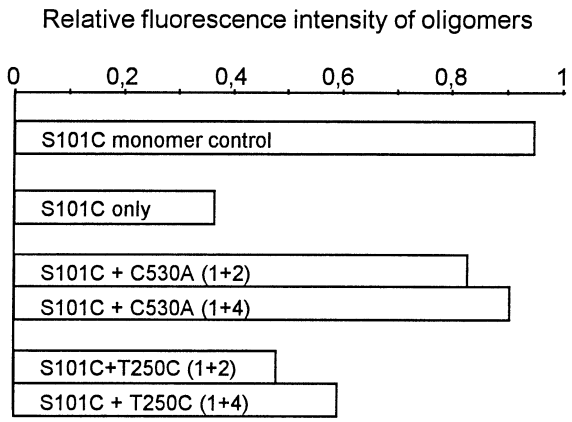

Fig. 4. T250C-AEDANS does not strictly cap growing oligomers. Purified oligomers of the active mutant S101C, thiol-specifically labeled with fluorescein maleimide, were assayed for fluorescein fluorescence before and after dissociation with SDS. The relative emission intensity (at 518 nm) of the undissociated oligomer was only ~40%, indicating that mutual contact of the fluorescein molecules attached to neighboring subunits had occurred. In contrast, when hybrid oligomers were generated of S101C-fluorescein and the unlabeled mutant C530A in excess, the quench was largely prevented due to the separation of labeled subunits by unlabeled ones. Although to a lesser extent, the quench was also relieved by T250C-AEDANS instead of C530A, showing that T250C-AEDANS may also assume an intervening position in the oligomer and is not confined to its free end as would be expected if a T250C-AEDANS subunit would entirely abrogate subsequent oligomerization.

contact surfaces. The findings reported so far might suggest that modification of T250C with IAEDANS blocks one of these sites. Addition of a T250C-AEDANS molecule to an oligomer via its functional contact surface would then leave the blocked surface exposed and hence terminate oligomerization (this mechanism is known to occur in the polymerization of actin and, aptly, has been termed 'capping'). Then, in a mixed oligomer, T250C-AEDANS should always assume a terminal position, and the rest of the oligomer should consist of a continuous stretch of active molecules. Alternatively, it is conceivable that T250C-AEDANS does not cause a total block but just a delay of subsequent oligomerization. In that case, T250C-AEDANS monomers should also occur at random positions along the hybrid oligomer. To differentiate between these possibilities, we employed the active mutant S101C thiol-specifically derivatized with fluorescein maleimide. Oligomerization of this protein is associated with a pronounced quenching of the fluorescence emission of the attached fluorescein molecules (Figure 4). The quench was largely absent in mixed oligomers of S101C-fluorescein and the equally active but unlabeled mutant C530A. This was expected, since the S101C-fluorescein monomers should be separated by intervening unlabeled C530A molecules in such mixed oligomers. The quench associated with oligomerization therefore depends on interaction of fluorescein molecules bound to adjacent oligomer subunits. When the same experiment was carried out with T250C-AEDANS instead of C530A, it was seen that, albeit to a lesser extent, T250C-AEDANS also diminished the fluorescence quench upon oligomerization. (Note that, at the excitation wavelength of 488 nm, T250C-AEDANS will not contribute fluorescence on its own.) Thus, like C530A, T250C-AEDANS had effected separation of S101C-fluorescein molecules, and its occurrence was not confined to the ends of oligomers. We conclude that addition of a T250C-AEDANS molecule obstructs but does not entirely block the subsequent process of oligomerization.

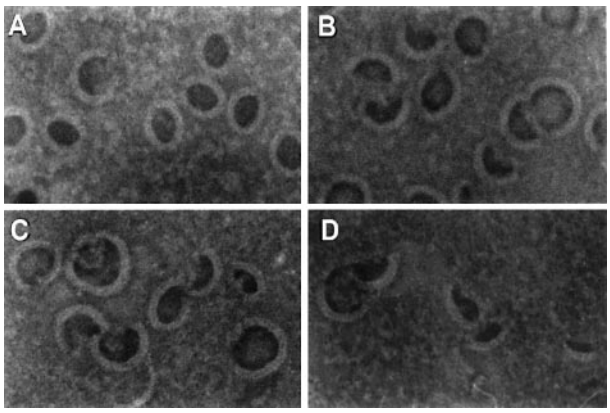

Fig. 5. Electron microscopy of hybrid oligomers. Hybrid oligomers of SLO mutants C530A and T250C-AEDANS were generated on rabbit erythrocytes. The membranes were washed and examined after negative staining with silicotungstate. Various molar ratios of the two mutants were employed. (**A**) Control sample with C530A only. The majority of the lesions are fully or almost fully circularized. (**B**) Equal amounts of both mutants, (**C**) 2-fold and (**D**) 4-fold excess of T250C-AEDANS over C530A. With increasing amounts of T250C-AEDANS, the average size of the oligomers was reduced, but the typical arc form as well as the crescent-shaped membrane defects were preserved.

Hybrid oligomers of reduced size are arc-shaped

On electron micrographs of toxin-treated erythrocyte membranes, the typical wild-type SLO oligomers appear as rings that are accompanied by some arcs (Bhakdi *et al.*, 1985). A very similar picture was obtained with the functional mutant C530A (Figure 5A). Adding increasing amounts of T250C-AEDANS progressively enhanced the number of incomplete arc-shaped lesions; fairly small arcs

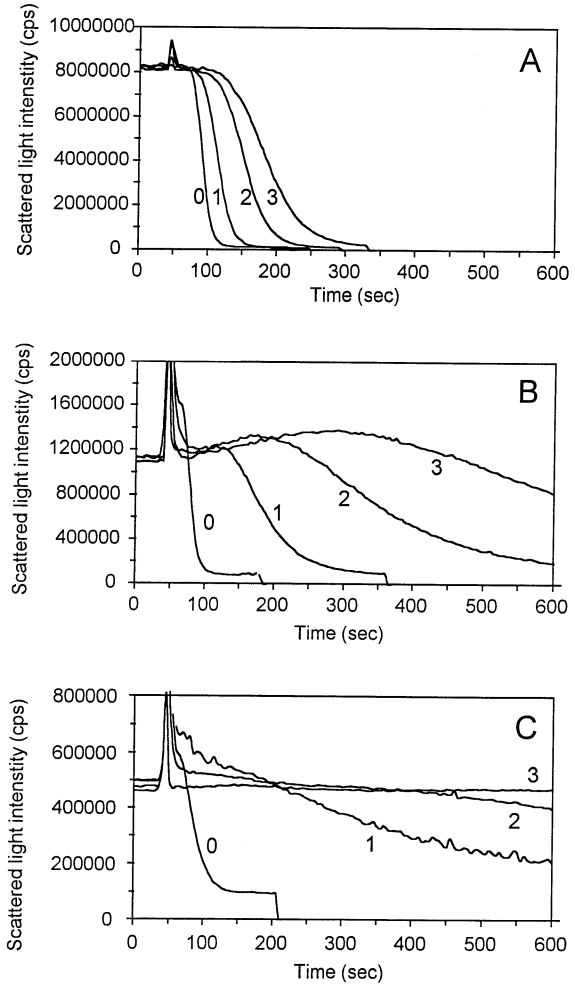

Fig. 6. Small hybrid oligomers form pores that are amenable to osmotic protection. Rabbit erythrocytes were suspended to 0.2% in buffered isotonic solutions of either (**A**) sodium chloride, (**B**) dextran 4 (4 kDa) or (**C**) dextran 60 (60 kDa). The cell suspension was stirred at 37°C, and its turbidity was monitored as a function of time in a fluorimeter. A constant amount (30 ng/ml) of SLO C530A supplemented with 0, 1, 2 or 3 times this amount of T250C-AEDANS was admixed; the respective molar ratio of T250C-AEDANS to C530A is indicated at the side of each curve (their upward spikes are artifacts due to opening of the sample chamber for addition of the toxin). While in saline the time course of hemolysis was only slightly retarded by addition of T250C-AEDANS, this delay was clearly more conspicuous with dextran 4. With a 3-fold excess of T250C-AEDANS over C530A and dextran 60, lysis was no longer apparent. This osmotic protection indicates that the pores in question were so small that they restricted permeation of the dextran molecules.

in the virtual absence of rings were obtained with a 4-fold excess of T250C-AEDANS (Figure 5B–D). Apart from their size, the hybrid oligomers show no morphological deviations from those of wild-type SLO.

Arc-shaped oligomers form pores of reduced functional diameter

Our hypothesis of concomitant oligomer assembly and pore formation predicts that an arc creates a membrane lesion that is reduced in functional size as compared with the ring. Osmotic protection experiments permit estimates of pore size to be made, and this method was applied next.

In the experiment of Figure 6, erythrocytes were suspended in isotonic solutions of sodium chloride, dextran 4 (mol. wt 4 kDa) or dextran 60 (60 kDa). The effective diameter of dextran 4 in solution is estimated to be 3 nm and that of dextran 60 to be 10 nm (Scherrer and Gerhardt, 1971). The cells were exposed to C530A toxin with or without T250C-AEDANS, and the time course of cell lysis was followed by measuring the decrease in turbidity of the cell suspension. Figure 6A shows the lysis of erythrocytes suspended in saline. It is seen that T250C-AEDANS effected no more than a slight delay of hemolysis. Figure 6B and C depicts the time course of hemolysis in the presence of dextran 4 or dextran 60, respectively. With increasing amounts of T250C-AEDANS, the rate of cell lysis was considerably reduced. This effect is more pronounced with dextran 60, which virtually abolished lysis of cells treated with T250C-AEDANS in 3-fold excess over C530A. In contrast, no major effect of the dextrans was seen with the samples containing C530A toxin only. This means that the hybrid pores are smaller than those of C530A alone, so that they restrict or prevent permeation of dextran molecules and, hence, osmotic cell lysis.

Comparison of experiments with different solutes is affected by the pronounced increase in viscosity caused by the addition of dextran in osmotically protective concentrations. We therefore also studied the release of fluorescent markers from resealed erythrocyte ghosts. Calcein (mol. wt 622 Da) was mixed with tetramethylrhodamine-labeled dextran (TMR-dextran; 4.4 or 76 kDa, respectively) and entrapped in erythrocyte ghosts. Serial dilutions were prepared from various mixtures of T250C-AEDANS and C530A toxins, and the labeled ghosts were added and incubated. After pelleting the membranes by centrifugation, the amount of marker released into the supernatant was determined fluorimetrically. With C530A alone and also with up to a 4-fold excess of T250C-AEDANS (Figure 7A–C), the release of calcein and of the smaller dextran species were closely matched, indicating that the pores formed did not discriminate between solutes with mol. wts of 0.6 and 4.4 kDa, respectively. With an 8-fold excess of T250C-AEDANS over C530A, however, a slight but reproducible difference in the release of both markers was apparent, indicating that a fraction of the pores formed now restricted the release of the dextran molecules. As expected, more pronounced effects were observed with the larger dextran molecules (76 kDa). Even with C530A alone (Figure 7F), there was a preferential release of calcein at partially lytic concentrations of the toxin. Addition of T250C-AEDANS further diminished the release of dextran molecules (Figure 7G and H); with an 8-fold excess of T250C-AEDANS, dextran release was virtually abolished (Figure 7I). Figure 7E and K shows that, at the highest concentrations employed, T250C-AEDANS rendered the resealed ghosts somewhat leaky towards small molecules. This did not seem to be the case with erythrocytes, which remained intact even at much higher dosages of the mutant toxin. Taken together, the findings of both osmotic protection and marker release experiments support the contention that SLO arcs constitute transmembrane pores, and that the functional pore diameter is related directly to the size of the arc.

Discussion

Oligomerizing, pore-forming proteins are important pathogenicity factors of many bacteria. Despite their diversity

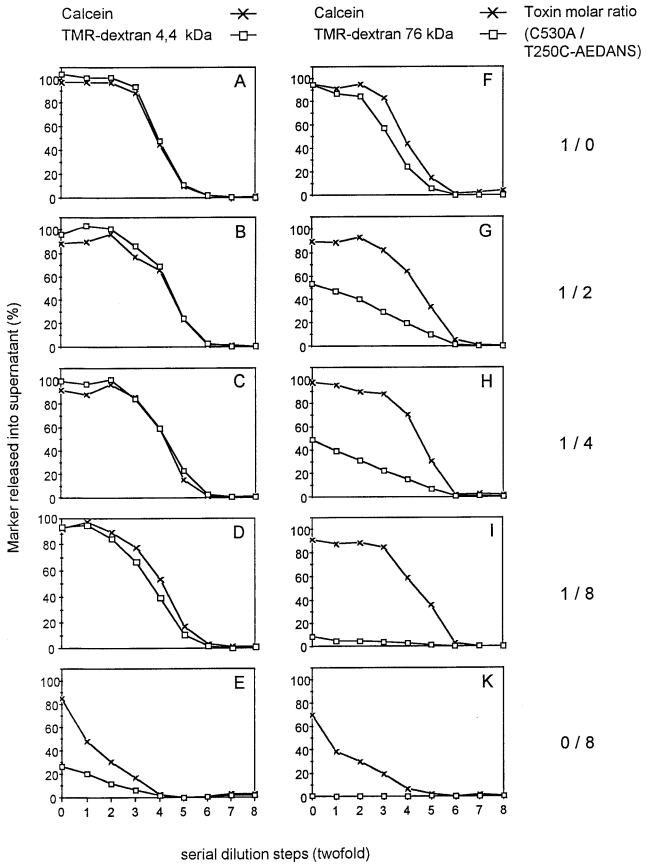

Fig. 7. Release of fluorescent markers through pores formed by small oligomers. Serial 2-fold dilutions of C530A toxin supplemented with varying amounts of T250C-AEDANS were prepared. At dilution step 0, the concentration of C530A toxin was 0.6 μg/ml in all experiments except those of (E) and (K); the amount of T250C-AEDANS is given as the molar ratio to C530A at the side of the panels. Resealed rabbit erythrocyte membranes laden with calcein (mol. wt 622 kDa) and tetramethylrhodamine-dextran (TMR-dextran; mol. wt 4.4 or 76 kDa, respectively) were added and incubated. After pelleting the membranes by centrifugation, the amounts of markers released into the supernatant were determined fluorimetrically. (**A–C**) The release of calcein and the smaller dextran species (left column) was indistinguishable at up to a 4-fold excess of T250C-AEDANS, so that the pores did not discriminate the two compounds by size. (**D**) With an 8-fold excess of T250C-AEDANS, there was a small but reproducible reduction in the release of dextran [15 ± 4% SD at dilution step 5, where there was no release of either marker due to T250C-AEDANS alone (**E**)]. This indicates exclusion of TMR-dextran from a fraction of the pores. (**F–I**) As expected, TMR-dextran of 76 kDa was retained more efficiently; (F) suggests that even with the active C530A toxin alone, a fraction of the pores is diminished in functional diameter.

in primary structure, these proteins form pores that are usually fairly small in diameter (1–2 nm), permitting flux of small molecules but not of proteins. This is the case with staphylococcal α-toxin (Fuessle *et al.*, 1981) and aerolysin (Parker *et al.*, 1994), the two most thoroughly studied pore-forming toxins. In both instances, cell-bound monomers diffuse on the membrane and oligomerize to form pre-pore structures in which the pore-forming domains remain outside the bilayer. Pore formation occurs subsequently via cooperative events, which result in membrane insertion of the critical amino acid sequences (Valeva *et al.*, 1996). In the case of α-toxin, a β barrel is formed that consists of 14 amphipathic β strands arranged into 7-fold rotational symmetry (Song *et al.*, 1996).

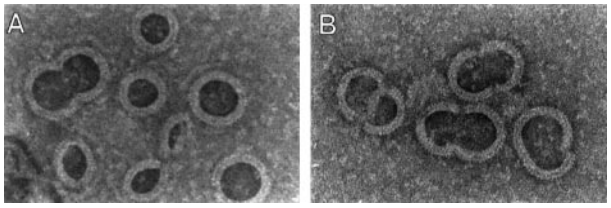

Fig. 8. Incomplete oligomers tend to form twin arcs on membranes. Electron micrograph of streptolysin O mutant C530A on liposome membranes. Several incomplete arc-shaped oligomers are arranged facing each other; their ends do not appear properly joined. The twin arcs are probably stabilized by the surface tension of the surrounding membrane.

Against this background, the family of thiol-activated toxins is unusual in that transmembrane pores of remarkable size (~30 nm in diameter) are created, each comprising a large number (~50–80) of subunits. A straightforward application of the above pre-pore mechanism (Figure 9A) to the thiol-activated toxins has been proposed (Rossjohn *et al.*, 1997), but this meets with conceptual difficulties. Thus, while simultaneous displacement of the membrane constituents in a lesion is conceivable with the small α-toxin pore, a huge energy barrier would have to be overcome in the case of the much larger defect created by SLO. Furthermore, control and coordination of the large number of subunits in simultaneous membrane insertion appears to be virtually impossible.

These difficulties are avoided in a different model of SLO pore assembly which we are advancing (Figure 9B). The model was based originally on electron microscopic observations (Bhakdi *et al.*, 1985) in conjunction with kinetic data on the oligomerization process (Palmer *et al.*, 1995), and has been corroborated further here.

Ultrastructural studies indicated that SLO lesions are heterogeneous in size. Along with fully circularized structures, arcs of widely different dimensions were observed on lysed erythrocyte membranes. The possibility that incomplete arc-shaped oligomers may create functional pores was suggested by indirect evidence: purified and reconstituted into liposomes, they appeared to form crescent-shaped membrane defects. The lesions seemed to be lined by the membrane-embedded protein arcs on the one hand, and by a free straight edge of the lipid bilayer on the other. The simplest explanation for these findings was that arcs and rings represented various stages of lesion formation, i.e. the membrane defects form at an early stage of oligomerization and grow in size concomitantly with addition of protomers to the arcs.

The hypothesis of simultaneous oligomer assembly and pore formation now gains strong support from the demonstration that incomplete arc-shaped oligomers indeed create functional holes in their target membranes. This was rendered possible by the availability of a chemically derivatized mutant of SLO (T250C-AEDANS) that, by interference with the oligomerization process, permitted the final size of the membrane lesion to be manipulated. This mutant does not appear to cause a total block but rather a delay of subsequent oligomerization. Nevertheless, its mode of action resembles the ‘capping’ of actin polymerization by an ADP-ribosylated actin derivative (Aktories and Wegner, 1992). Like the latter molecule, SLO T250C-AEDANS is incapable of initiating oligo-

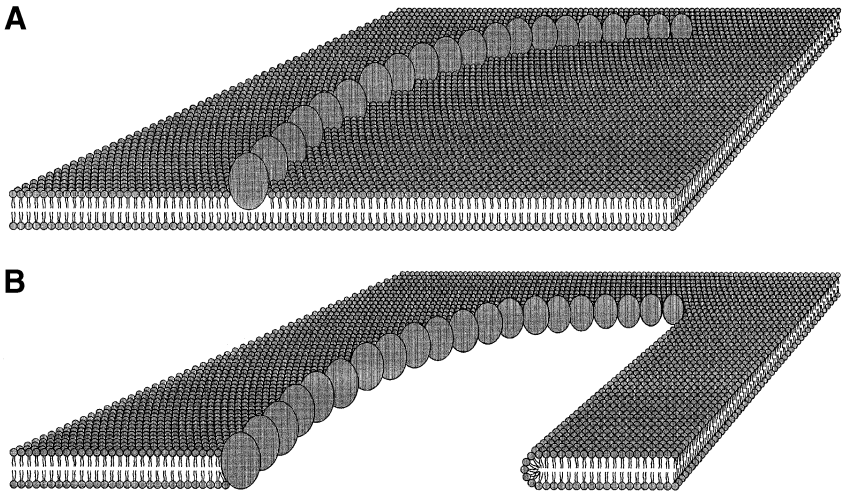

Fig. 9. Hypothetical intermediates in the assembly of the streptolysin O pore. (**A**) Formation of the perfringolysin O pore has been proposed to involve an arc-shaped oligomeric intermediate that is not yet inserted into the membrane (Rossjohn *et al.*, 1997) and, accordingly, should not create a membrane lesion. (**B**) In contrast, we propose that the oligomer is membrane-inserted from the very beginning, so that a small oligomer creates a transmembrane pore that is faced on the opposite side by a free edge of the membrane (Bhakdi *et al.*, 1985).

merization. Both proteins, however, may join a growing oligomer of active subunits and thereby exert their inhibitory effects. With SLO, this is important as an independent confirmation of the actin-like two-step oligomerization mechanism that has been inferred from kinetic analysis (Palmer *et al.*, 1995).

Within the context of the proposed mechanism of pore formation, a consideration of physico-chemical aspects is warranted. Granted the basic assumption that membrane insertion occurs at an early stage of the oligomer, we can plausibly account for the simultaneous initiation of the membrane lesion. Like the inner circumference of a fully assembled ring, the concave surface of an inserted arc must be ascribed a hydrophilic character. Deprived of favorable hydrophobic interaction with this protein surface, the adjacent membrane lipids will become subject to surface tension and hence retract to form the edge facing the arc that is visualized by electron microscopy. With arcs reconstituted into liposomes, this edge appears as a straight line (Bhakdi *et al.*, 1985), which would yield the maximum relaxation of surface tension. The shape of the lipid edge seems somewhat more varied in the case of arc lesions on erythrocytes. Conceivably, the protein scaffold underneath the erythrocyte membrane interferes with the ideal arrangement of the lipids, although we do not exclude the possibility that the edges become distorted by the OsO_4 fixation step of the electron microscopy sample preparation procedure. In any case, the reality of surface tension at free edges of the membrane is illustrated nicely by a phenomenon commonly seen with toxin-treated erythrocytes or liposomes: twin arcs positioned ends-on (Figure 8). These twin arcs apparently are not held together by regular protein contacts. Instead, their stability derives from relieving the membrane of two free edges. Accordingly, twin arcs are no longer observed once the membrane is dissolved with detergent (Bhakdi *et al.*, 1985).

An interesting question that cannot yet be answered conclusively relates to the exact minimum size of the oligomer sufficient for pore initiation. The fact that with a large excess of T250C-AEDANS over C530A there is some differential permeation of calcein and dextran molecules as small as 4.4 kDa (or 3 nm) suggests that very small pores may be formed which consist of very few, possibly only two or three, subunits. It is tempting to speculate that the pore is initiated right at the start of oligomerization, which we have proposed to consist of the formation of a dimer (Palmer *et al.*, 1995). Attempts are underway to investigate whether a membrane-inserted dimer creates a functional lesion.

Taken together, the collective results are relevant for a number of reasons. They provide quite compelling evidence for the lesion extension model of SLO pore assembly. They demonstrate how functionally altered toxin mutants can be created and used to manipulate pore size. This will provide cell biologists with novel reagents to effect controlled plasma membrane permeabilization. Perhaps most importantly, the data indicate that transmembrane pores may in some cases be lined only partially by proteins, with lipids forming the rest of the pore wall. A conceptually related situation has been reported for the protein-conducting channel in the protein translocation machinery of the endoplasmatic reticulum. There, it was shown that the protein-conducting channel is open laterally towards the lipid bilayer, such that the signal or signal anchor sequence initially faces the lipid bilayer, whereas the hydrophilic translocating portion is in a proteinaceous environment (Martoglio *et al.*, 1995). Conceivably, similar slits in the membrane created by inserting amino acid sequences may also serve to translocate intracellularly acting toxin components (e.g. diphtheria toxin A; Montecucco *et al.*, 1992; Eriksen *et al.*, 1994) across membranes.

Materials and methods

Production of chemically derivatized, mutant proteins

Site-directed mutagenesis (Cormack, 1987), protein expression and purification (Weller *et al.*, 1996), and labeling of purified mutant proteins with fluorescein maleimide (Palmer *et al.*, 1993) were done as described. Labeling with IAEDANS was carried out in the same way as with fluorescein maleimide, except that the reagent was dissolved to 100 mM in 1 M Tris–HCl pH 8.0 and employed at 10 mM final concentration. The respective labeling yields were determined as described in Valeva

et al. (1996). Thiol-specific labeling of the active mutant N218C with ^{125}I using fluorescein maleimide as a carrier was done as described (Palmer *et al.*, 1997).

Hemolytic titration

Serial 2-fold dilutions of the mutant proteins were prepared in a microtiter plate with phosphate-buffered saline (PBS)/0.1% bovine serum albumin (BSA). To each dilution, an equal volume of rabbit erythrocytes (2.5% by vol.) was admixed. The plates were incubated at 37°C for 30 min before visual reading of the hemolytic titer.

Binding of IAEDANS-labeled SLO T250C to rabbit erythrocytes

To verify that the IAEDANS-labeled SLO mutant T250C (SLO T250C-AEDANS) binds to rabbit erythrocytes, the protein was dissolved at 5 μg/ml in PBS/0.1% BSA, and rabbit erythrocytes were added to 5% by vol. The sample was left on ice for 5 min to allow for binding, and the cells were then pelleted by centrifugation. The fraction of unbound toxin in the supernatant was determined fluorimetrically, whereby a control sample to which no red cells had been added served as a reference.

Electron microscopy

SLO mutant C530A (Pinkney *et al.*, 1989) was admixed with varying amounts (see Results) of SLO T250C-AEDANS. Then 25 μg of the protein mixture was added to 500 μl of rabbit erythrocytes (10% by vol. in 20 mM HEPES, 125 mM NaCl, 0.1% BSA) and incubated at 37°C for 15 min. At this stage, the samples were completely hemolytic. The erythrocyte membranes were obtained by centrifugation (10 min, 10 000 *g*, 4°C). The pellet was washed twice in the former buffer. Samples were fixed with OsO_4 and mounted for electron microscopy with silico-tungstate negative staining as described (Bhakdi *et al.*, 1985). Liposomes, prepared from bovine brain lipids (Fluka) and cholesterol (25% by weight) according to Mayer *et al.* (1986), were incubated with the toxins as above and mounted without fixation.

Characterization of hybrid oligomers by density gradient centrifugation

Oligomerization was induced from mixtures of C530A and T250C-AEDANS mutant proteins as above, except that a small amount of active radiolabeled mutant S218C (~10^5 c.p.m. per sample) was included to facilitate subsequent quantitation of oligomers. The toxin-lysed samples were solubilized with deoxycholic acid [final concentration 5% (w/v)] and subjected to sucrose density gradient centrifugation in the presence of deoxycholate essentially as described (Bhakdi *et al.*, 1985). Briefly, the samples were layered on top of 10–50% sucrose gradients supplemented with 0.25% deoxycholate and centrifuged for 1 h at 50 000 r.p.m. and 4°C in a Beckman VTI-65-2 vertical rotor. Ten fractions were harvested from the bottom of gradients, and the radioactivity per volume was determined to obtain the distribution of SLO among the gradient fractions.

Characterization of hybrid oligomers by gel permeation chromatography

The IAEDANS-labeled mutant proteins (200 μg) were allowed to oligomerize for 30 min at 37°C on sonicated liposomes (prepared according to Valeva *et al.*, 1996; 2.5 mg total lipid, molar cholesterol content 40%). The samples were solubilized by adding Triton X-100 to 0.5% and chromatographed over a Sephacryl S300 column (16 mm× 60 cm) equilibrated with 20 mM Tris, 100 mM NaCl and 0.1% Triton X-100 (pH 8.3). Fractions of 2.8 ml were collected and analyzed for label fluorescence.

Quantitation of oligomerization-associated fluorescence quenching

The SLO mutant S101C (Palmer *et al.*, 1996), labeled with fluorecein maleimide, was admixed to either C530A or T250C-AEDANS (amounts as indicated in Results) and incubated at 37°C with washed membranes of osmotically lysed rabbit erythrocytes. The membranes were solubilized with deoxycholate and centrifuged as above, and the bottom three density gradient fractions were pooled and passed over a Sepharose 6B column (operated as the S300 column above). The isolated oligomers were assayed for fluorescein fluorescence. Upon dissociation of the oligomers by incubation with SDS (0.5%) at 70°C for 5 min, the fluorescence was measured again, and the relative fluorescence intensity of the oligomers obtained as the quotient of the two measurements.

Spectrofluorimetry

All samples were examined in an SPEX Fluoromax spectrofluorimeter with bandpasses set to 2.1 or 4.2 nm. To detect the fluorescence of IAEDANS-labeled proteins, the following wavelength settings were used: excitation, 338 nm; emission, 440–540 nm. For fluorescein, the excitation wavelength was 488 nm, while the emission was recorded between 500 and 540 nm. The emission of supernatants from the marker release experiments (see below) was assayed at 572 nm with excitation between 480 and 560 nm; the intensities at 492 and 552 nm (divided by those of a positive control; below) were taken as the amounts of released calcein and TMR-dextran, respectively. All spectra were subtracted with the appropriate buffer blanks.

Osmotic protection experiments

A standard buffer (10 mM sodium phosphate, 25 mM NaCl, 0.5 mg/ml BSA, pH 7.5) was supplemented with either dextran 4 (9 g/100 ml), dextran 60 (12 g/100 ml) or 100 mM NaCl (these concentrations were found to provide similar osmotic protection to erythrocytes). Washed rabbit erythrocytes were made up in the former buffers to 0.2% (v/v). 3 ml of the erythrocyte suspensions were stirred in a quartz cuvette thermostatted at 37°C inside the fluorimeter. The excitation and emission wavelengths of the instrument were set to 620 nm, and the scattered light emanating from the turbid erythrocyte suspension was monitored as a function of time. After 2 min, various mixtures of SLO mutants C530A and T250C-AEDANS (as stated in Results) were admixed. Incubation was continued until the intensity of scattered light had dropped to a stable level and hemolysis was complete, or for a maximum of 15 min.

Marker release experiments

Washed, packed human erythrocytes were lysed on ice with 10 vol. of 10 mM HEPES/NaOH (pH 7.5) and repeatedly washed by centrifugation (4°C at 15 000 *g* for 3 min) in the same buffer. After a final wash with 10 mM HEPES/140 mM NaCl (HBS), the ghosts were resuspended in the same buffer containing 15 μM calcein [bis(carboxymethyl)aminomethyl-fluorescein; Sigma] and 0.25 mg/ml of TMR-dextran (Sigma; average mol. wts, 4.4 or 76 kDa, respectively) and incubated at 37°C for 45 min. The resealed ghosts were washed four times with HBS, incubated for 30 min on ice, and washed again. The pellet was then resuspended in 20 vols of the same buffer. C530A toxin (0.6 μg/ml) was admixed with various amounts (see Results) of T20C-AEDANS, and serial 2-fold dilutions thereof were prepared in 100 μl of HBS supplemented with 0.5 mg/ml BSA. To these samples, 50 μl of the above ghost suspension were added, followed by incubation at 37°C for 30 min. The samples were then centrifuged at 12 000 *g* for 2 min, and the supernatants were diluted into 3 ml of 10 mM Tris/50 mM NaCl/0.2% SDS (pH 8.0) and analyzed fluorimetrically. The percentage of release of either marker was obtained by comparison with a Triton-lysed reference; spontaneous leakage was assayed on a parallel sample without toxin and subtracted.

Acknowledgements

We thank Silvia Weis for skilful technical assistance and El Moeiz Abdel Ghani for critically reading the manuscript. This work was supported by the Deutsche Forschungsgemeinschaft (grant Pa-539/1).

References

Aktories,K. and Wegner,A. (1992) Mechanisms of the cytopathic action of actin-ADP-ribosylating toxins. *Mol. Microbiol.*, **6**, 2905–2908.

Alouf,J.E. and Geoffroy,C. (1991) The family of antigenically related, cholesterol-binding ('sulphhydryl-activated') cytolytic toxins. In Alouf,J.E. and Freer,J.H. (eds), *Sourcebook of Bacterial Protein Toxins*. Academic Press, London, pp. 147–186.

Bhakdi,S. and Tranum Jensen,J. (1984) Mechanism of complement cytolysis and the concept of channel-forming proteins. *Philos. Trans. R. Soc. Lond. Biol.*, **306**, 311–324.

Bhakdi,S., Tranum Jensen,J. and Sziegoleit,A. (1985) Mechanism of membrane damage by streptolysin-O. *Infect. Immun.*, **47**, 52–60.

Bhakdi,S., Weller,U., Walev,I., Martin,E., Jonas,D. and Palmer,M. (1993) A guide to the use of pore-forming toxins for controlled permeabilization of cell membranes. *Med. Microbiol. Immunol.*, **182**, 167–175.

Cormack,B. (1987) Mutagenesis by the polymerase chain reaction. In Ausubel,F.M., Brent,R., Kingston,R.E., Moore,D.M., Seidman,J.G., Smith,J.A. and Struhl,K. (eds), *Current Protocols in Molecular Biology*. Wiley & Sons, New York.

Eriksen,S., Olsnes,S., Sandvig,K. and Sand,O. (1994) Diphtheria toxin at low pH depolarizes the membrane, increases the membrane conductance and induces a new type of ion channel in Vero cells. *EMBO J.*, **13**, 4433–4439.

Fuessle,R., Bhakdi,S., Sziegoleit,A., Tranum Jensen,J., Kranz,T. and Wellensiek,H.J. (1981) On the mechanism of membrane damage by *Staphylococcus aureus* alpha-toxin. *J. Cell Biol.*, **91**, 83–94.

Hugo,F., Reichwein,J., Arvand,M., Kramer,S. and Bhakdi,S. (1986) Use of a monoclonal antibody to determine the mode of transmembrane pore formation by streptolysin O. *Infect. Immun.*, **54**, 641–645.

Martoglio,B., Hofmann,M.W., Brunner,J. and Dobberstein,B. (1995) The protein-conducting channel in the membrane of the endoplasmic reticulum is open laterally toward the lipid bilayer. *Cell*, **81**, 207–214.

Mayer,L.D., Hope,M.J. and Cullis,P.R. (1986) Vesicles of variable sizes produced by a rapid extrusion procedure. *Biochim. Biophys. Acta*, **858**, 161–168.

Montecucco,C., Papini,E., Schiavo,G., Padovan,E. and Rossetto,O. (1992) Ion channel and membrane translocation of diphtheria toxin. *FEMS Microbiol. Immunol.*, **5**, 101–111.

Ohno Iwashita,Y., Iwamoto,M., Mitsui,K., Ando,S. and Iwashita,S. (1991) A cytolysin, theta-toxin, preferentially binds to membrane cholesterol surrounded by phospholipids with 18-carbon hydrocarbon chains in cholesterol-rich region. *J. Biochem., Tokyo*, **110**, 369–375.

Palmer,M., Jursch,R., Weller,U., Valeva,A., Hilgert,K., Kehoe,M. and Bhakdi,S. (1993) *Staphylococcus aureus* alpha-toxin. Production of functionally intact, site-specifically modifiable protein by introduction of cysteine at positions 69, 130, and 186. *J. Biol. Chem.*, **268**, 11959–11962.

Palmer,M., Valeva,A., Kehoe,M. and Bhakdi,S. (1995) Kinetics of streptolysin O self-assembly. *Eur. J. Biochem.*, **231**, 388–395.

Palmer,M., Saweljew,P., Vulicevic,I., Valeva,A., Kehoe,M. and Bhakdi,S. (1996) Membrane-inserting domain of streptolysin O identified by cysteine scanning mutagenesis. *J. Biol. Chem.*, **271**, 26664–26667.

Palmer,M., Buchkremer,M., Valeva,A. and Bhakdi,S. (1997) Cysteine-specific radioiodination of proteins with fluorescein maleimide. *Anal. Biochem.*, **253**, 175–179.

Parker,M.W., Buckley,J.T., Postma,J.P., Tucker,A.D., Leonard,K., Pattus,F. and Tsernoglou,D. (1994) Structure of the *Aeromonas* toxin proaerolysin in its water-soluble and membrane-channel states. *Nature*, **367**, 292–295.

Pinkney,M., Beachey,E. and Kehoe,M. (1989) The thiol-activated toxin streptolysin O does not require a thiol group for cytolytic activity. *Infect. Immun.*, **57**, 2553–2558.

Rossjohn,J., Feil,S.C., McKinstrey,W.J., Tweten,R.K. and Parker,M.W. (1997) Structure of a cholesterol-binding, thiol-activated cytolysin and a model of its membrane form. *Cell*, **89**, 685–692.

Scherrer,R. and Gerhardt,P. (1971) Molecular sieving by the *Bacillus megaterium* cell wall and protoplast. *J. Bacteriol.*, **107**, 718–735.

Sekiya,K., Satoh,R., Danbara,H. and Futaesaku,Y. (1993) A ring-shaped structure with a crown formed by streptolysin O on the erythrocyte membrane. *J. Bacteriol.*, **175**, 5953–5961.

Song,L., Hobaugh,M.R., Shustak,C., Cheley,S., Bayley,H. and Gouaux,J.E. (1996) Structure of staphylococcal alpha-hemolysin, a heptameric transmembrane pore. *Science*, **274**, 1859–1866.

Valeva,A., Weisser,A., Walker,B., Kehoe,M., Bayley,H., Bhakdi,S. and Palmer,M. (1996) Molecular architecture of a toxin pore: a 15-residue sequence lines the transmembrane channel of staphylococcal alpha-toxin. *EMBO J.*, **15**, 1857–1864.

Valeva,A., Palmer,M. and Bhakdi,S. (1997) Staphylococcal α-toxin: formation of the heptameric pore is partially cooperative and proceeds through multiple intermediate stages. *Biochemistry*, **36**, 13298–13304.

Walker,B., Krishnasastry,M., Zorn,L. and Bayley,H. (1992) Assembly of the oligomeric membrane pore formed by staphylococcal alpha-hemolysin examined by truncation mutagenesis. *J. Biol. Chem.*, **267**, 21782–21786.

Weller,U. *et al.* (1996) Expression of active streptolysin O in *Escherichia coli* as a maltose binding protein–streptolysin O fusion protein: the N-terminal 70 amino acids are not required for hemolytic activity. *Eur. J. Biochem.*, **236**, 34–39.

Received January 5, 1998; revised January 23, 1998; accepted January 26, 1998